

## Nonconservative sandpile models

Peyman Ghaffari,<sup>1</sup> Stefano Lise,<sup>2</sup> and Henrik Jeldtoft Jensen<sup>1,\*</sup>

<sup>1</sup>*Department of Mathematics, Imperial College 180 Queen's Gate, London SW7 2BZ, United Kingdom*

<sup>2</sup>*SISSA/ISAS Via Beirut 2-4, 34014 Trieste, Italy*

(Received 14 August 1996; revised manuscript received 2 July 1997)

We study the effect of nonconservation in two sandpilelike models by means of mean-field considerations, numerical simulations (in two dimensions), and by a renormalization-group (RG) analysis. We find, in agreement with previous studies, that criticality is lost in the randomly driven nonconservative models. Our main objective is to understand this result in terms of the branching ratio of the avalanche dynamics and from the view point of a RG analysis. The distribution of avalanches is found numerically to follow a stretched exponential with a cutoff that diverges as the conservative case is approached. The behavior of the cutoff is reproduced by the RG analysis. We conclude that uniform drive is a necessary—but not sufficient—condition for critical behavior in the nonconservative regime. [S1063-651X(97)13112-9]

PACS number(s): 64.60.Ht, 05.40.+j, 05.70.Jk

### I. INTRODUCTION

A clear understanding of the *conditions* necessary for SOC is still lacking. Conservation was thought of as being crucial for the existence of a critical state [1,2]. It has been shown [3,4] that introducing dissipation in the original sandpile models destroys criticality. On the other hand, the numerical so-called earthquake model introduced by Olami, Feder, and Christensen (OFC) proved that a critical state can exist even when the updating algorithm does not conserve the dynamical variable [5]. The criticality observed in this nonconservative model has been ascribed to a marginal synchronization by several authors [6,7]. Although synchronization is definitely of importance to the existence of a critical state in the OFC model, we found in a recent study that synchronization is not a necessary condition [8]. This conclusion followed from a study of a random neighbor version of the OFC model. Synchronization is completely destroyed by the assignment of random neighbors at each update. Nevertheless, the model exhibits power laws for a range of conservation levels.

In the present paper, we try to gain some insight along two different approaches: first, by a mean-field calculation of the branching ratio and second, by a renormalization-group (RG) calculation. The advantage of the mean-field treatment is that it allows a simple physical interpretation of why criticality is lost when dissipation is introduced. For a similar methodological purpose we find it important to investigate to what extent the RG method developed by Díaz-Guilera for conservative SOC models [9] can yield useful insight when applied to nonconservative models.

In our previous study of the OFC model, we found that the branching ratio  $\sigma$  (to be defined below) could be used as a single parameter measure of whether the model exhibits critical or noncritical behavior. When  $\sigma < 1$ , we found the random neighbor model to be noncritical. Correspondingly, when  $\sigma = 1$  we found that the model exhibits power law

behavior [10]. It is obviously important to know if the branching ratio can be trusted as a discriminator between critical and noncritical behavior in models of SOC.

In the more technically involved language of the RG discussion one sees that criticality is lost because the globally attractive fixed point of the conservative theory is repulsive along the directions in parameter space that correspond to the nonconservative terms in the equation of motion. One moves towards the conservative fixed point when the dissipation level is tuned to zero. As this is done the correlation length will diverge as some inverse power  $\nu$  of the conservation level. The RG calculation allows us to calculate this exponent. The situation is the following. We find numerically that the distribution of avalanches behaves like  $s^{-a} \exp[-(s/s_0)^b]$ , where  $a \approx 1$ ,  $b \approx 1.3$ , and  $s_0 \sim (1/q_c - \alpha)^{-2\nu}$  with  $\nu \approx 1/2$ . Here  $\alpha$  is the dissipation parameter and  $q_c$  the coordination number,  $\alpha = 1/4$  corresponds to the conservative case. The RG analysis predicts  $\nu = 1/\mu_{max}$ , where  $\mu_{max} = d_i^\gamma - d_i^\lambda = 2$  is the largest eigenvalue at the conservative fixed point and  $d_i^\gamma$  ( $d_i^\lambda$ ) are the scaling dimensions of the nonconservative (conservative) operators.

In the present paper we focus on two models. One is a slightly modified version of the cellular automaton model used by Bak, Tang, and Wiesenfeld (BTW), where they introduced the concept of self-organized criticality (SOC) [11]. The second model is a nonconservative version of a model introduced by Zhang [12]. Our conclusion from the study to be presented below is that only the Zhang model can remain critical in the nonconservative regime and only if the model is uniformly driven, in which case the model is identical to the OFC model.

The difference between the *uniformly driven* BTW model studied numerically in the present paper and the OFC model consists only in the way the dynamical variable of an overcritical site is transferred to neighboring sites. This difference turns out to be of the greatest importance. The uniformly driven OFC model exhibits criticality at a finite level of nonconservation. In contrast, the BTW model becomes noncritical as soon as one breaks the conservation, and this happens for either mode of drive (random or uniform).

The paper is organized the following way. We define the

\*Author to whom correspondence should be addressed. Electronic address: h.jensen@ic.ac.uk

models in the next section. In Sec. III we present a mean-field discussion of the behavior of the model as dissipation is introduced. Section IV contains our numerical simulations of the random neighbor as well as of the nearest neighbor version of the model. In Sec. V we describe a dynamical renormalization-group analysis of a Langevin equation. In this analysis we attempt to take into account the threshold criterion by including the Heaviside step function in the Langevin equation. Section VI contains a discussion and conclusions.

## II. DEFINITION OF MODEL

The two models we consider are defined in terms of a real dynamical variable  $E(\mathbf{r},t)$ , where  $\mathbf{r}$  denotes a site on a  $d$ -dimensional cubic lattice. In order to fix our terminology, we will call  $E(\mathbf{r},t)$  the energy. The initial configuration is chosen at random. The dynamical evolution of the field  $E(\mathbf{r},t)$  is controlled by a threshold  $E_c$ . When all sites have field values  $E(\mathbf{r},t) \leq E_c$  energy is added to the system from the outside. The energy can be added in two ways.

(1) *Uniform drive*. In this case all sites grow at the same rate

$$\frac{dE(\mathbf{r},t)}{dt} = \bar{\eta} \quad (1)$$

until one of the sites hits the threshold value  $E_c$ .

(2) *Random drive*. In this case one adds an amount  $\delta E$  to a randomly chosen site  $\mathbf{r}$ :

$$E(\mathbf{r},t) \rightarrow E(\mathbf{r},t) + \delta E. \quad (2)$$

The procedure continues until one of the sites exceeds the threshold value  $E_c$ .

When the energy of one of the sites of the lattice becomes larger than the threshold value, the driving is switched off and the system relaxes according to one of the following two rules.

(a) The (generalized) BTW model:

$$\begin{aligned} E(\mathbf{r},t) > E_c \rightarrow E(\mathbf{r},t+1) &= E(\mathbf{r},t) - E_c \rightarrow E(\mathbf{r}_n, t+1) \\ &= E(\mathbf{r}_n, t) + \alpha E_c. \end{aligned} \quad (3)$$

(b) The Zhang model:

$$\begin{aligned} E(\mathbf{r},t) > E_c \rightarrow E(\mathbf{r},t+1) &= 0 \rightarrow E(\mathbf{r}_n, t+1) = E(\mathbf{r}_n, t) \\ &+ \alpha E(\mathbf{r},t). \end{aligned} \quad (4)$$

Here  $\mathbf{r}_n$  denotes the set of neighbor sites assigned to the site  $\mathbf{r}$ . The lattice is updated simultaneously. The relaxation is continued until the energy on all sites  $\mathbf{r}$  is below the threshold value  $E(\mathbf{r},t) \leq E_c$  once again. When this happens one switches back to the appropriate driving mode (uniform or random) and adds energy to the system.

The constant  $\alpha$  determines the conservation level. When  $\alpha < 1/q_c$ , where  $q_c$  is the coordination number of the lattice, an amount equal to  $(1 - \alpha q_c)\mathcal{E}$  is lost as a consequence of the update, where  $\mathcal{E} = E_c$  for the generalized BTW model and  $\mathcal{E} = E(\mathbf{r},t)$  for the Zhang model. For our numerical simula-

tions we use open boundary conditions. When  $\mathbf{r}_n$  denotes a site outside the boundary of the system, the energy transferred to this site is lost.

We want to make a few comments concerning the relation between the models described above and previously studied models. The conservative version ( $\alpha = 1/q_c$ ) of the generalized BTW model driven randomly, i.e., mode (2), is similar to the original BTW sandpile cellular automaton [11] in the way the energy of an overcritical site is transferred. Namely, a fixed amount  $E_c$  is removed from the site and a corresponding amount  $q_c \alpha E_c$  is isotropically transferred to the neighboring sites. This is close in spirit to the BTW dynamics, where, due to the discrete nature of the variable  $q_c$ , ‘‘units’’ are removed from the active site. When the Zhang model is driven uniformly, i.e., mode (1), the model is identical to the OFC model. In contrast to the BTW-like model, the total energy  $E(\mathbf{r},t)$  is removed in this model and an amount proportional to it, namely,  $q_c \alpha E(\mathbf{r},t)$ , is distributed.

The generalized BTW model is different from the original BTW model in that we allow  $E(\mathbf{r},t)$  to assume real values rather than only integer values. BTW updated their model by adding an amount  $\delta E$  ( $=1$ ) to randomly chosen sites. We use in our simulations below a spatial homogeneous drive as in the model by OFC [5]. This is done in order to investigate whether or not the uniform drive will enable the model to remain critical in the nonconservative regime ( $\alpha < 1/q_c$ ). We find that even the uniformly driven BTW model is noncritical when the relaxation is nonconservative. Our mean-field discussion in the next section illuminates why the generalized BTW model behaves so differently from the Zhang model.

## III. MEAN-FIELD ARGUMENT

Let us consider a random-neighbor version of the generalized BTW model. Instead of distributing the energy to a fixed set of nearest-neighbor sites, a new collection of  $q_c$  random neighbors are chosen in each update. This is a convenient way to eliminate the effect of spatial correlations. The random-neighbor model is therefore expected to be more applicable to a mean-field description than is the original nearest-neighbor model.

The random-neighbor version of the sandpile model was solved by Christensen and Olami [13] by recognizing the close relation to a branching process. The mapping of random-neighbor models onto independent branching processes has turned out to be very illuminating. In our recent study of the OFC model [8], we found the branching ratio to be a useful indication of criticality. In the following we adapt the previous analysis to the present model. We are aware that in the present case our considerations will essentially reduce to the arguments of Ref. [13]. However, we believe that our reasoning makes the significance of the parameter  $\alpha$  more apparent.

The branching ratio  $\sigma$  is defined as the ratio  $n(t+1)/n(t)$  between the number of overcritical sites at two consecutive updates during the evolution of the avalanches. An average over the avalanche evolution as well as over different realizations of avalanches is performed:

$$\sigma = \langle n(t+1)/n(t) \rangle. \quad (5)$$

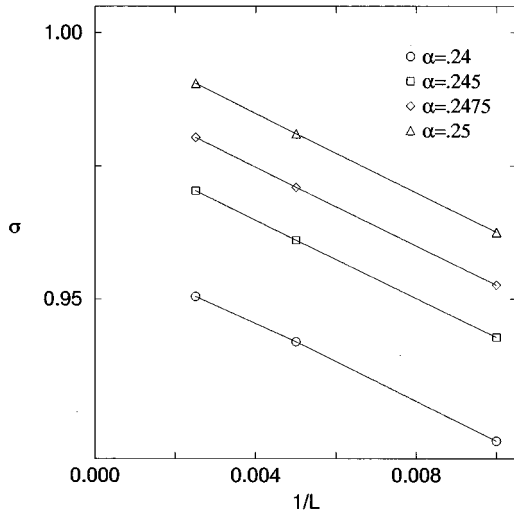


FIG. 1. Branching ratio in the random-neighbor model as a function of  $1/L$  ( $L=100,200,400$ ), for different values of  $\alpha$ . From bottom to top,  $\alpha=0.24, 0.245, 0.2475, 0.25$ .

Let  $P_+$  denote the probability that a random site becomes overcritical as an effect of receiving  $\alpha E_c$  from an updated overcritical site.  $P_+$  is simply the probability that the  $E$  value of a site is between  $E_c - E_c \alpha$  and  $E_c$ :

$$P_+ = \int_{(1-\alpha)E_c}^{E_c} dE P(E), \quad (6)$$

where  $P(E)$  is the probability that the  $E$  field of a site will assume the value  $E$ . It can be shown [13] that the distribution  $P(E)$  is uniform on the interval  $[0, E_c]$ . Accordingly, we get  $P_+ = \alpha$  and for the branching ratio

$$\sigma = q_c P_+ = q_c \alpha. \quad (7)$$

We expect the model to be critical only when  $\sigma = 1$ . This implies  $\alpha = 1/q_c$ . Thus criticality is lost according to this argument when the model becomes nonconservative.

Our numerical simulations of the random-neighbor version of the generalized BTW model indeed confirm the conclusion of this mean-field argument. We find that the avalanche size distribution has the form

$$P(s) \propto s^{(-3/2)} \exp(-s/s_0)$$

and that  $s_0$  diverges as  $(1/q_c - \alpha)^{-2}$  as  $\alpha \rightarrow 1/q_c$ , in agreement with Ref. [13]. The measured branching ratio as a function of  $1/L$  is shown in Fig. 1 for different values of  $\alpha$ . One observe that only for  $\alpha = 1/4$  does  $\sigma$  extrapolate to 1 as  $L \rightarrow \infty$ .

A similar calculation for the Zhang update [Eq. (4)] gives  $P_+ = \alpha \langle E^+ \rangle / E_c$  and therefore  $\sigma_{Zh} = q_c \alpha \langle E^+ \rangle / E_c$ , where  $\langle E^+ \rangle$  denotes the average energy of the relaxing overcritical sites [8]. We notice that the Zhang model may be able to keep  $\sigma_{Zh} \geq 1$  when  $\alpha \in [\alpha_c, 1/q_c]$ . Here,  $\alpha_c = E_c / (q_c \langle E^+ \rangle)$  is smaller than  $1/q_c$  because the supercritical amount of energy  $E^+ > E_c$ . This cannot happen during the BTW update [Eq. (3)], where a fixed amount  $\alpha E_c$  is passed on to the neighboring sites independent of the values of the field  $E(\mathbf{r}, t)$  at the overcritical site.

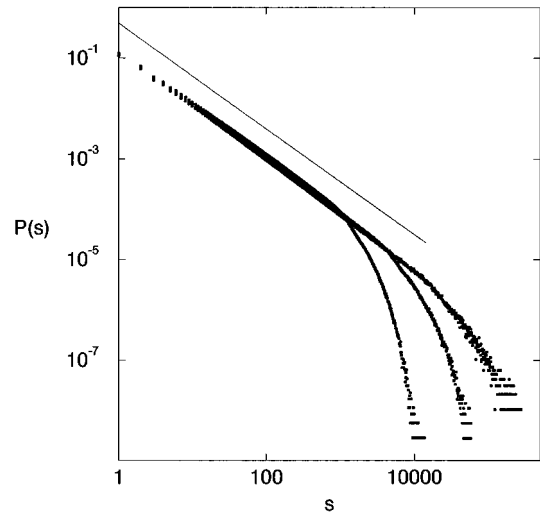


FIG. 2. Avalanche size distribution for  $\alpha=0.25$  and  $L=50, 100$ , and  $200$ . The slope of the distribution is slightly larger than 1,  $\tau \sim 1.05$ .

The equivalent mean-field arguments applied to the OFC model [8] predicted  $\alpha_c = 2/(2q_c + 1)$ . In two dimensions, where  $q_c = 4$ ,  $\alpha_c = 2/9$ , in surprisingly good agreement with our simulations of the random-neighbor version of the OFC model.

To summarize, the mean-field arguments suggest that  $\sigma < 1$  for the nonconservative sandpile model defined by Eq. (3). Hence, we expect criticality to be lost as soon as  $\alpha < 1/q_c$ . This finding is in agreement with our simulations of the nearest-neighbor version of the generalized BTW model to be presented in the next section.

#### IV. SIMULATION RESULTS

We present in this section the results of two-dimensional simulations of the generalized BTW model defined in Eq. (3), with nearest-neighbor interactions and driven uniformly according to Eq. (1). For  $\alpha = 1/4$  the avalanche size distributions scales with system size, as can be seen in Fig. 2. This is the hallmark of criticality. On the other hand, for  $\alpha < 1/4$ , no scaling with system size is observed for sufficiently large systems. A level of dissipation as small as 1 part in 1000 is enough to destroy criticality, see Fig. 3. The characteristic length scale of the system (measuring roughly the maximum size of an avalanche) grows for increasing values of  $\alpha$ . We have tentatively tried to describe the behavior of the system (in the regime of  $\alpha$  values close to  $1/q_c$ ) by fitting the avalanche distributions to the stretched exponential form  $P(s) \sim s^{-a} \exp[-(s/s_0)^b]$ . The fits are shown as lines in Fig. 4. We use  $a = 1$  and  $b = 1.3$  for all values of  $\alpha$ . The characteristic avalanche size  $s_0$  diverges as  $\alpha \rightarrow (1/4)^-$ . Figure 5 shows a fit to the behavior  $s_0 \sim (1/4 - \alpha)^{-2\nu}$ , where  $\nu = 1/2$ . Hence, our simulations show that the nearest-neighbor model, like the random-neighbor model, ceases to be critical as soon as  $\alpha$  is made smaller than  $1/q_c$ . In the next section we present renormalization-group arguments that illuminate this numerical finding and allows us to understand the value  $\nu = 1/2$ .

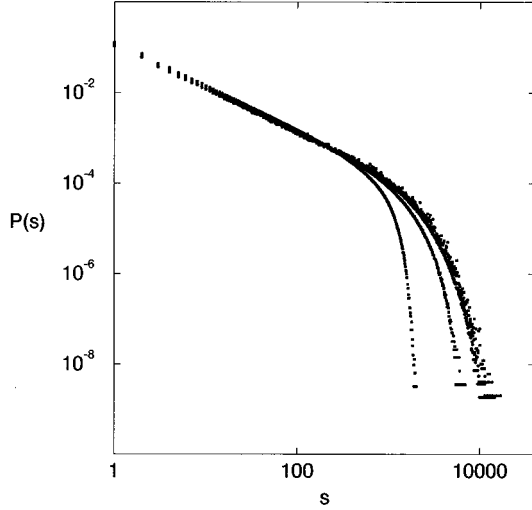


FIG. 3. Avalanche size distributions for  $\alpha=0.24975$ . The distributions refer to systems of linear size  $L=50$ ,  $L=100$ ,  $L=200$ , and  $L=400$ . No finite size scaling is present for  $L>200$ .

### V. RENORMALIZATION-GROUP ANALYSIS

In order to apply the dynamical renormalization-group (DRG) analysis to the dynamics of the models defined by the update in Eqs. (3) and (4), it is convenient to rewrite the algorithm in the following form:

$$E(\mathbf{r}, t+1) = E(\mathbf{r}, t) - \mathcal{E}\Theta(E(\mathbf{r}, t) - E_c) + \sum_{\mathbf{r}_n} \alpha \mathcal{E}\Theta(E(\mathbf{r}_n, t) - E_c) + \eta_d(\mathbf{r}, t). \quad (8)$$

The sum runs over the neighbor sites  $\mathbf{r}_n$  of the site  $\mathbf{r}$ . The value of the symbol  $\mathcal{E}$  depends on which of the two models we consider. For the generalized BTW model [see Eq. (3)] we have  $\mathcal{E}=E_c$ . For the Zhang model [see Eq. (4)] we have  $\mathcal{E}=E(\mathbf{r}, t)$ . The time  $t$  refers to the lattice updates and  $\Theta(x)$  is the step function:  $\Theta(x)=0$  for  $x \leq 0$  and  $\Theta(x)=1$  for  $x > 0$ .

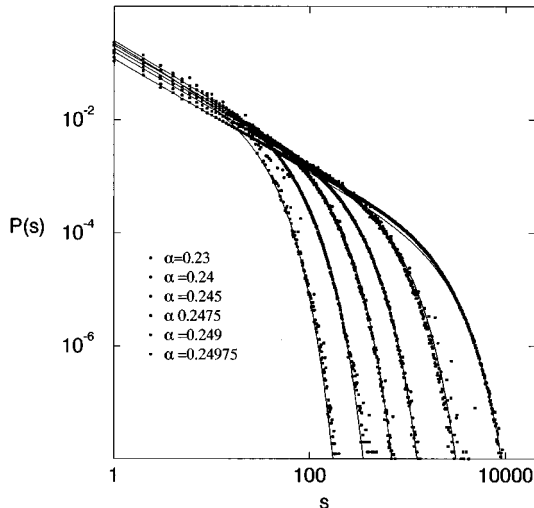


FIG. 4. Avalanche size distributions for  $\alpha < 0.25$ . The continuous lines are fits of the form  $P_\alpha(s) \propto s^{-1} \exp[-(s/s_0)^{1.3}]$ .

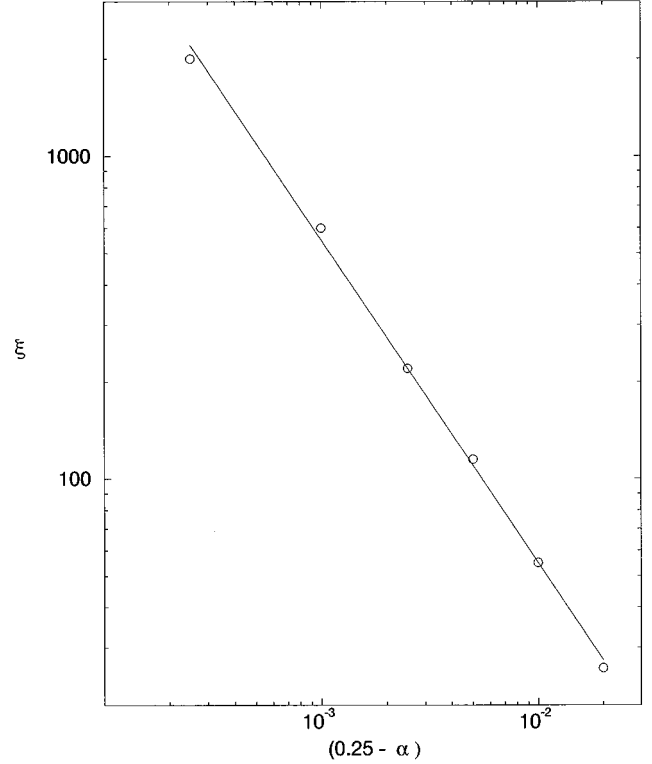


FIG. 5. Cutoff in avalanche size distribution  $s_0$  as a function of  $(0.25 - \alpha)$ . The solid line is the interpolation  $s_0 \sim (0.25 - \alpha)^{-1}$ .

We have introduced a source term  $\eta_d(\mathbf{r}, t)$  to represent the driving of the system. The uniform drive [case (1) above] can be represented by the following expression:

$$\eta_d(\mathbf{r}, t) = \eta_0 \prod_{\mathbf{r}} \Theta(E_c - E(\mathbf{r}, t)). \quad (9)$$

One notes that the drive acts with the same strength  $\eta_0$  at all sites. Moreover, the drive only acts whenever *all* sites have  $E$  values below the threshold value. The random drive can correspondingly be represented by

$$\eta_d(\mathbf{r}, t) = \eta(\mathbf{r}, t) \prod_{\mathbf{r}} \Theta(E_c - E(\mathbf{r}, t)), \quad (10)$$

where  $\eta(\mathbf{r}, t)$  is a white noise signal in space and time.

The continuum limit of Eq. (8) is given by the following equation:

$$\partial_t E(\mathbf{r}, t) = [\alpha \tilde{D} \nabla^2 + (\alpha q_c - 1)] \Theta(E(\mathbf{r}, t) - E_c) \mathcal{E} + \eta_d(\mathbf{r}, t), \quad (11)$$

where  $\tilde{D}$  is an undetermined phenomenological diffusion constant arising from the coarse-graining procedure involved when deriving Eq. (11). The form of the drive in Eqs. (9) and (10) makes it difficult to apply standard RG techniques. Díaz-Guilera has suggested that the random drive [see Eq. (10)] can be represented by a much simpler expression [14]. Let us now explain this idea. We choose to write the source in the form

$$\eta_d(\mathbf{r}, t) = \bar{\eta} + \eta(\mathbf{r}, t), \quad (12)$$

where  $\langle \eta(\mathbf{r}, t) \rangle = 0$ . Since the drive only acts in between the avalanches and the lifetime of the avalanches spans all time scales we may try to capture the time correlations in the drive defined in Eq. (10) by assuming the following correlator for the fluctuating part of the drive:

$$\langle \eta(\mathbf{r}, t) \eta(\mathbf{r}', t') \rangle = 2\Gamma \delta^d(\mathbf{r} - \mathbf{r}'). \quad (13)$$

It should be noted that this expression only corresponds to the usual white noise correlator for the spatial degrees of freedom. The correlator is assumed to be independent of time. This is supposed to represent that the drive only acts in between the avalanches. This feature of the noise correlator leads to a critical dimension  $d_c = 4$  for the conservative theory, in agreement with general expectation [14,15]. The standard noise, which is  $\delta$  correlated in both time and space, leads to  $d_c = 2$ .

Neglect for a moment the fluctuating part of the drive by assuming  $\eta_d(\mathbf{r}, t) = \bar{\eta}$ . Consider the limit of slow driving  $\bar{\eta} \ll (1 - \alpha q_c) E_c$ . A second thought will convince the reader that any spatially homogeneous time-dependent solution to Eq. (11),  $E(\mathbf{r}, t) = E(t)$ , will evolve towards the time-independent solution  $E(t) = \lim_{\epsilon \rightarrow 0^+} (E_c + \epsilon)$ . This observation leads us to look for solutions of the form

$$E(\mathbf{r}, t) = E_c + \delta E(\mathbf{r}, t), \quad (14)$$

where  $\delta E(\mathbf{r}, t)$  has zero average.

To make the Langevin equation in Eq. (11) suitable for the standard RG analysis, we need to regularize the nonanalytical behavior of the step function [9,16,17]. We think that the details of the analysis are interesting and useful, but since they are of a somewhat technical nature we have deferred these details to the Appendix. The idea of the calculation is to study the fixed point structure of the Langevin equation as more and more nonlinearities are included in the representation of the step function. We only succeed in applying the RG calculation in the case of the random drive [Eq. (10)]. In this case we conclude that the BTW model and the Zhang model are equivalent even in the nonconservative regime. We do not find any attractive fixed points for either model when  $\alpha < 1/q_c$ . In order to understand how critical behavior develops as  $\alpha \rightarrow 1/q_c$ , we study the stability matrix of the conservative fixed point when nonconservation is included. The correlation length diverges according to  $\xi \sim (1/q_c - \alpha)^{-\nu}$ . We determine the value of  $\nu$  from the largest eigenvalue,  $\mu_{max}$  of the stability matrix. The result is  $\nu = 1/\mu_{max} = 1/2$ .

This result is in agreement with the numerical simulations where the characteristic avalanche size  $s_0$  scales as  $s_0 \sim (1/4 - \alpha)^{-1}$  in two dimensions (see Sec. IV and Ref. [3]). In two dimensions we know that avalanches are compact [24] and therefore expect  $s_0$  to scale as  $\xi^2$ . Generally we would expect

$$s_0 \sim \xi^{D_f} \sim (1/q_c - \alpha)^{-\nu D_f} \sim (1/q_c - \alpha)^{D_f/2}, \quad (15)$$

where  $D_f$  is the fractal dimension of the avalanche.

## VI. DISCUSSION AND CONCLUSIONS

We have studied the effect of lack of conservation in two types of algorithms and for two different types of drive. One updated algorithm consists of a BTW-like update in which a fixed amount is distributed to the neighboring sites during a relaxation update of an overcritical site. The other update rule we have analyzed is of the type considered by Zhang [12] and by OFC [5] in which an amount proportional to the energy of the relaxing site is distributed during the relaxation. We distinguish between models driven by energy packages added at random sites or a uniform drive in which all sites increases their energy with the same constant rate. We addressed the question: Can the uniformly driven BTW model stay critical in the nonconservative regime? The answer is no.

This lack of robustness with respect to the introduction of a nonconservative element in the update algorithm is to be contrasted with the behavior of the OFC model [5,8]. This model remains definitely critical when a low level of dissipation is introduced. The only difference between the uniformly driven version of the BTW model we have studied and the OFC model is in the way an overcritical site distributes energy to its neighbor sites. In our model the active site relaxes to  $E - E_c$  and distributes the fixed amount  $q_c \alpha E_c$ . In the OFC model the active site relaxes to zero and distributes an amount  $q_c \alpha E$ . We believe this difference to be important in two ways. The variable amount of energy distributed in the OFC algorithm together with the resetting of the relaxing site to  $E = 0$  allow the synchronization of the sites [6]. Moreover, an effective conservation can occur during the avalanche in the OFC model because the quantity  $q_c \alpha E$  can be greater than  $E_c$  even for  $\alpha < 1/q_c$ .

We have determined numerically the cutoff  $s_0$  in the avalanche distribution. We find that  $s_0 \sim (a_c - \alpha)^{-2\nu}$ , where  $\nu \approx 1/2$ . Since avalanches are compact in two dimensions we conclude that the correlation length of the model diverges as  $\xi \sim (a_c - \alpha)^{-\nu}$  when the conservative limit  $\alpha \rightarrow \alpha_c = 1/q_c$  is approached. This result is in agreement with a previous study by Manna, Kiss, and Kertész [3] of a slightly different randomly driven model. We stress that  $\nu \approx 1/2$  is found numerically for the BTW-like model for the uniform as well as for the random drive.

We have presented a renormalization-group analysis from which we conclude that the randomly driven BTW and the Zhang models are equivalent and both cease to exhibit critical behavior in the nonconservative regime. This result is an extension of a previous result for the conservative case by Díaz-Guilera [9]. From our RG analysis we find that  $\nu = 1/2$  for dimensions less than  $d_c = 4$ . This agrees well with the numerical result mentioned in the paragraph above. The exponent  $\nu$  has also been calculated by Vespignani, Zapperi, and Pietronero [25]. They find that  $\nu \approx 0.67$  in two dimensions. Their result depends, however, on the size of their coarse-graining cell in their real-space renormalization procedure and the value estimate for  $\nu$  by Vespignani *et al.* has a tendency to decrease with increasing size of the coarse-graining cell [26]. It is not clear why our RG result  $\nu = 1/2$  for the randomly driven BTW model should agree with the numerical simulation of the uniformly driven BTW model. The reason might be, as suggested by numerical simulations,

that the randomly driven and the uniformly driven BTW models have identical exponents  $\nu$ .

When we studied the uniformly driven random-neighbor version of the Zhang or OFC model we found that the critical conservation value is  $\alpha_c \approx 2/9$  and that the corresponding exponent is  $\nu \approx 3/2$  [8]. From this we conclude that (for reasons that are not clear to us at the moment) the BTW model uniformly driven behaves as the RG analysis of the randomly driven version of the model predicts, whereas the same is not the case for the uniformly driven Zhang (or OFC) model.

The overall conclusion of our paper is the following. Uniform drive (in contrast to random drive) is a necessary condition for critical behavior in the nonconservative regime. But uniform drive is not a sufficient condition. The synchronization and effective energy conservation allowed by the Zhang update [8] appears to be necessary in addition to the uniform drive in order to obtain critical behavior in nonconservative sandpilelike models.

#### ACKNOWLEDGMENTS

H.J.J. is grateful to Kim Christensen for very helpful discussions.

#### APPENDIX: RG ANALYSIS

This appendix contains some of the nonstandard features of applying the RG method to Eq. (11). First, we need to find a way to represent the step function in terms of a (infinite) polynomial [9,16,17]. Consider a real function  $f: \mathfrak{R} \rightarrow \mathfrak{R}$  with the following properties: (a)  $\lim_{x \rightarrow -\infty} f(x) = 0$ , (b)  $\lim_{x \rightarrow \infty} f(x) = 1$ , and (c) the function can be expanded around  $x = 0$  and has infinite radius of convergence. The step function is represented by

$$\Theta(x) = \lim_{\beta \rightarrow \infty} f(\beta x). \quad (\text{A1})$$

From Eqs. (11), (14), and (A1) we derive

---


$$\partial_t E(\mathbf{r}, t) = D \nabla^2 E + \lambda_2 \nabla^2 E^2 + \lambda_3 \nabla^2 E^3 + \lambda_4 \nabla^2 E^4 + \lambda_5 \nabla^2 E^5 + \dots + \gamma_1 E + \gamma_2 E^2 + \gamma_3 E^3 + \gamma_4 E^4 + \gamma_5 E^5 + \dots + \eta(\mathbf{r}, t). \quad (\text{A5})$$

where  $\langle E \rangle = \langle \eta \rangle = 0$  [to simplify the notation we have dropped the  $\delta$  in front of  $E(\mathbf{r}, t)$ , see Eq. (A2)]. The coefficients for the generalized BTW model and the Zhang model are given, respectively, by

$$D \equiv \lambda_1 = \frac{\alpha \tilde{D} E_c \beta}{\sqrt{\pi}} \quad \text{or} \quad \alpha \tilde{D} \left( \frac{1}{2} + \frac{E_c \beta}{\sqrt{\pi}} \right), \quad \gamma_1 = (\alpha q_c - 1) \frac{E_c \beta}{\sqrt{\pi}} \quad \text{or} \quad (\alpha q_c - 1) \left( \frac{1}{2} + \frac{E_c \beta}{\sqrt{\pi}} \right), \quad \lambda_2 = 0 \quad \text{or} \quad \frac{\alpha \tilde{D} \beta}{\sqrt{\pi}},$$

$$\gamma_2 = 0 \quad \text{or} \quad \frac{(\alpha q_c - 1) \beta}{\sqrt{\pi}}, \quad \lambda_3 = - \frac{\alpha \tilde{D} E_c \beta^3}{3 \sqrt{\pi}} \quad (\text{same for the Zhang model}),$$

$$\gamma_3 = - (\alpha q_c - 1) \frac{E_c \beta^3}{3 \sqrt{\pi}} \quad (\text{same for the Zhang model}), \quad \text{etc.} \quad (\text{A6})$$

$$\begin{aligned} \partial_t \delta E(\mathbf{r}, t) &= \lim_{\beta \rightarrow \infty} [\alpha \tilde{D} \nabla^2 + (\alpha q_c - 1)] \\ &\times f(\beta \delta E(\mathbf{r}, t)) \mathcal{E} + \eta_d(\mathbf{r}, t). \end{aligned} \quad (\text{A2})$$

The part of the equation independent of  $\delta E(\mathbf{r}, t)$  can be removed from the equation by the following specific tuning of the constant part of the drive,

$$\bar{\eta} = (1 - \alpha q_c) E_c, \quad (\text{A3})$$

where we imagine that the limit  $\beta \rightarrow \infty$  is followed by the limit  $\delta E \rightarrow 0$ . We believe that this tuning represents the implicit tuning which, in fact, occurs during simulations of the model. One recalls that the model is *not* driven during the evolution of the avalanches. This allows the model to act at a point where the energy added to the model in between the avalanches is precisely balanced by the energy dissipated during the avalanche. In the simulations of the model, dissipation takes place in the bulk when  $\alpha < 1/q_c$  (dissipation always occurs at the open boundary of the system), and Eq. (A3) represents the same type of balance.

Our next step is to choose the function  $f(x)$  in Eq. (A2). We use in our concrete calculations the probability integral [18]

$$\begin{aligned} f(x) &= \frac{1}{\sqrt{\pi}} \int_{-\infty}^x dt e^{-t^2} \\ &= \frac{1}{2} + \frac{1}{\sqrt{\pi}} \sum_{k=1}^{\infty} (-1)^{k+1} \frac{x^{2k-1}}{(2k-1)(k-1)!}. \end{aligned} \quad (\text{A4})$$

The results obtained for a specific choice of  $\Theta$ -function representation  $f(x)$  will not depend on  $f(x)$  when all terms in the expansion of  $f(x)$  are included and the limit  $\beta \rightarrow \infty$  is performed [16]. Substituting the expansion of the  $\Theta$  function into Eq. (A2) leads to the following equation:

Nonlinearities corresponding to even powers of the field  $E(\mathbf{r}, t)$  are absent in the BTW model but present in the Zhang model. The coefficients of the odd term are identical in the two models from three up. Note that  $\gamma_i \propto (\alpha q_c - 1)$  for all  $i$ , that is, in the conservative case all the  $\gamma_i$  terms disappear.

We now study the nature of the fixed point structure of Eq. (A5) by applying the usual RG procedure [19–21]. A transparent and clear explanation of the method can be found in [22]. Here we limit our discussion to the results of the analysis. We study the fixed point structure as more and more nonlinearities are included in Eq. (A5). To appreciate the potential of this approach it is worthwhile to mention that for the conservative case (i.e., all  $\gamma_i = 0$ ) the following happens [9]. The equation with  $\lambda_i = 0$  for all  $i \geq 3$  has no attractive fixed point in dimensions  $d < d_c = 4$ . However, an attractive fixed point appears for  $d < d_c$  when nonlinearities of higher than quadratic order is included. Thus it seems possible to describe the self-organization (attractive fixed point) produced by the threshold condition [15] (modeled by the  $\Theta$  function) by including a sufficient number of nonlinearities in Eq. (A5).

The difference between the set of nonlinearities that enters into the equation of motion for the BTW model and the Zhang model turns out to be irrelevant in the limit  $\beta \rightarrow \infty$ . This was shown by Díaz-Guilera for the conservative case [9]. In the nonconservative case the renormalization of the noise is different in the two models for finite  $\beta$  values. In the BTW model the strength of the noise correlator  $\Gamma$  in Eq. (13) is not renormalized. In the Zhang, however,  $\Gamma$  is renormalized at the one-loop level (including up to cubic nonlinearities) by a term proportional to the square of the nonconservative coupling constant  $\gamma_2$ . First, since  $\gamma_2$  vanishes in the conservative limit  $\alpha \rightarrow 1/q_c$ , we recover Díaz-Guilera's result in this limit. Second, the term responsible for the renormalization of  $\Gamma$  is proportional to  $\beta^{-2}$  and vanishes accordingly in the limit  $\beta \rightarrow \infty$ .

The following heuristic argument appears to be a simple way to see that the difference between the parity of the nonlinearities which enter into the equation of motion for the two models (BTW: odd terms only; Zhang: both odd and even) cannot represent a factual difference between the two models. Assume we represent the  $\Theta$  function in terms of Eq. (A1) by choosing a function  $f(x)$  which when expanded only contains odd powers of  $x$  [as in the example in Eq. (A4)]. The function  $x \mapsto [f(x)]^2$  will also be able to serve as a representation of the  $\Theta$  function. However,  $f^2(x)$  will contain both odd and even powers of  $x$ . Hence, if we make use of  $f^2(x)$  as our representation of the  $\Theta$  function in Eq. (A2) the BTW model and the Zhang model would not differ with respect to the oddness or evenness of the nonlinearities entering into Eq. (A5).

We conclude that the randomly driven BTW and the Zhang models remain equivalent even in the nonconservative case. These general considerations were confirmed when we analyzed Eq. (A5) by successively including nonlinearities up to fifth order. Let us now turn to the uniformly driven models. Numerical simulations show that the BTW model and the Zhang model *are* different when driven homoge-

neously. The criticality of the BTW model is destroyed as soon as any degree of nonconservation is introduced by choosing  $\alpha < 1/q_c$ . Whereas the Zhang model (which when driven homogeneously is identical to the OFC model) remains critical even for  $\alpha < 1/q_c$ .

Can the behavior of the uniformly driven models be understood by use of the RG technique? Can the homogeneously driven system [see Eq. (9)] be represented by a simple effective noise along the lines of Eqs. (12) and (13)? For instance, can we detect any trace of the appearance of an all-attractive fixed point for the RG flow equations when we damp the fluctuations in the noise by letting  $\Gamma \rightarrow 0$  in Eq. (13)? One could imagine that a difference between the two models could be detected in the limit where the fluctuations in the driving term  $\eta(\mathbf{r}, t)$  are made smaller by decreasing  $\Gamma$ . We were, however, unable to find any tendency towards a difference in the fixed point behavior of the two models in the limit of small  $\Gamma$ . We conclude that the nature of the drive must be treated more carefully in order to understand the difference between the two *uniformly* driven models by means of the RG approach.

Let us now explain how the value of the critical exponent  $\nu = 1/2$  can be understood in terms of the RG analysis. We first note that the coefficients  $\gamma_i$  and the coefficients  $\lambda_i$  originates from the expansion of the same function, namely the  $\Theta$  function. It seems therefore natural to assume that the identities

$$\frac{\gamma_i}{\gamma_j} = \frac{\lambda_i}{\lambda_j} \quad (\text{A7})$$

remain correct under renormalization. By use of this assumption we can deduce that the RG flow equations for the coupling constants are of the following form:

$$\begin{aligned} \frac{d\lambda_i}{d\ell} &= \lambda_i [F_i(\vec{\lambda}, \vec{\gamma}, \Gamma) + d_i^\lambda] \equiv h_i^\lambda, \\ \frac{d\gamma_i}{d\ell} &= \gamma_i [F_i(\vec{\lambda}, \vec{\gamma}, \Gamma) + d_i^\gamma] \equiv h_i^\gamma. \end{aligned} \quad (\text{A8})$$

We have made use of the following notation.  $F_i$  denotes a set of functions [to be calculated in principle through the loop expansion of Eq. (A5)]. The same function  $F_i$  enters the flow equation for  $\lambda_i$  and for  $\gamma_i$ . The functions  $F_i$  depends on the coupling constants  $\vec{\lambda} = (\lambda_1, \lambda_2, \dots)$  and  $\vec{\gamma} = (\gamma_1, \gamma_2, \dots)$ , and on the strength of the noise correlator  $\Gamma$ . The bare scaling dimension of the coupling constants are easily determined by dimensional analysis [19–22].

$$d_i^\lambda = (i-1)\chi + z - 2, \quad d_i^\gamma = (i-1)\chi + z = d_i^\lambda + 2. \quad (\text{A9})$$

Here we made use of the usual definitions of exponents: assume we scale space according to  $\mathbf{r} \rightarrow e^\ell \mathbf{r}$ . To compensate for this change of scale, we scale time and the field according to  $t \rightarrow e^{z\ell} t$  and  $E \rightarrow e^{\chi\ell} E$ . This defines the dynamical exponent  $z$  and the roughening exponent  $\chi$ .

The fixed points of the flow equations are obtained by demanding that all right hand sides in Eq. (A8) vanish simul-

taneously, i.e.,  $h_i^\lambda = h_i^\gamma = 0$  for all  $i$ . The conservative fixed point  $\vec{\lambda}^*$ , analyzed by Díaz-Guilera, is obtained by assuming that  $\vec{\gamma} = 0$  and then solving

$$F_i(\vec{\lambda}, 0, \Gamma) + d_i^\lambda = 0 \Rightarrow \vec{\lambda} = \vec{\lambda}^*. \quad (\text{A10})$$

This fixed point is attractive in the space consisting of the coupling constants  $\vec{\lambda}$ . We now study the stability of this fixed point in the larger coupling space consisting of  $\vec{\lambda} \otimes \vec{\gamma}$ . The linear stability of the fixed point  $(\vec{\lambda}, \vec{\gamma}) = (\vec{\lambda}^*, 0)$  is controlled by the Jacobian matrix

$$\partial h_{i(\vec{\lambda}^*, 0)} = \begin{pmatrix} \partial h_i^\lambda / \partial \lambda_j & \partial h_i^\lambda / \partial \gamma_j \\ \partial h_i^\gamma / \partial \lambda_j & \partial h_i^\gamma / \partial \gamma_j \end{pmatrix}_{(\vec{\lambda}^*, 0)} \quad (\text{A11})$$

$$= \begin{pmatrix} \frac{\lambda_i \partial(F_i)}{\partial \lambda_j} & \frac{\partial F_i}{\lambda_i \partial \gamma_j} \\ 0 & \delta_{ij}(F_i + d_i^\gamma) \end{pmatrix}_{(\vec{\lambda}^*, 0)}. \quad (\text{A12})$$

The diagonality of the partial derivatives  $\partial h_i^\gamma / \partial \gamma_j$  evaluated at the fixed point  $(\vec{\lambda}^*, 0)$  together with the identity

$$F_i(\vec{\lambda}^*, 0, \Gamma) = -d_i^\lambda, \quad (\text{A13})$$

which follows from Eq. (A10) makes it easy to see that the eigenvalues  $\mu$  of the Jacobian matrix in Eq. (A12) are determined by the following equation:

$$\det(\partial h - \mu I) = \det(\{\partial h_i^\lambda / \partial \lambda_j\} - \mu I) \prod_k (d_k^\gamma - d_k^\lambda - \mu) = 0. \quad (\text{A14})$$

Since  $\{\partial h_i^\lambda / \partial \lambda_j\}$  is simply the stability matrix of the Díaz-Guilera fixed point we conclude that the fixed point  $(\vec{\lambda}^*, 0)$  remains (as expected) attractive along the directions of the coupling constants  $\lambda_i$  and that the fixed point is repulsive along the directions  $\gamma_i$ . The eigenvalues of the repulsive directions are according to Eq. (A14) and Eq. (A9), all given by

$$\mu = d_i^\gamma - d_i^\lambda = 2. \quad (\text{A15})$$

As the fixed point  $(\vec{\lambda}^*, 0)$  is approached by tuning  $\alpha$  towards the critical value  $1/q_c$  (where all are the  $\gamma$  coupling constants vanish), the correlation length of the system will diverge according to

$$\xi \sim (1/q_c - \alpha)^{-\nu}, \quad (\text{A16})$$

where the exponent  $\nu$  is given by the inverse of the largest repulsive eigenvalue of the fixed point [23]. Hence in our case we have  $\nu = 1/2$ . This result is independent of dimension.

- 
- [1] G. Grinstein, D.-H. Lee, and S. Sachdev, Phys. Rev. Lett. **64**, 1927 (1990).
- [2] T. Hwa and M. Kadar, Phys. Rev. Lett. **62**, 1813 (1989).
- [3] S. S. Manna, L. B. Kiss, and J. Kertész, J. Stat. Phys. **61**, 923 (1990).
- [4] C. J. Pérez, Á. Corral, A. Díaz-Guilera, K. Christensen, and A. Arenas, Int. J. Mod. Phys. B **10**, 1111 (1996).
- [5] Z. Olami, H. J. S. Feder, and K. Christensen, Phys. Rev. Lett. **68**, 1244 (1992).
- [6] A. A. Middleton and C. Tang, Phys. Rev. Lett. **74**, 742 (1995).
- [7] Á. Corral, C. J. Pérez, A. Díaz-Guilera, and A. Arenas, Phys. Rev. Lett. **74**, 118 (1995).
- [8] S. Lise and H. J. Jensen, Phys. Rev. Lett. **76**, 2326 (1996). After this paper was completed we received analytical studies by M.-L. Chabanol and V. Hakim (adap-org/9706003) and by H.-M. Bröker and P. Grassberger (adap-org/9707002) that suggest that  $\alpha_c$  is, in fact, equal to  $1/q_c$  in the random-neighbor OFC model.
- [9] A. Díaz-Guilera, Europhys. Lett. **26**, 177 (1994).
- [10] Simulations of the nearest-neighbor OFC model also finds  $\sigma = 1$ . However, it is difficult to obtain good statistics when  $\alpha$  becomes small.
- [11] P. Bak, C. Tang, and K. Wiesenfeld, Phys. Rev. Lett. **59**, 381 (1987).
- [12] Y.-C. Zhang, Phys. Rev. Lett. **63**, 470 (1989).
- [13] K. Christensen and Z. Olami, Phys. Rev. E **48**, 3361 (1993).
- [14] A. Díaz-Guilera, Phys. Rev. A **45**, 8551 (1992), studied Eq. (A5) for  $\lambda_3 = 0$  and in Ref. [17] the more general  $\lambda_2 \neq 0$  and  $\lambda_3 \neq 0$  case was analyzed.
- [15] H. J. Jensen, *Self-Organized Criticality* (Cambridge University Press, Cambridge, in press).
- [16] P. Ghaffari and H. J. Jensen, Europhys. Lett. **35**, 397 (1996). Note that this paper contains a misprint: the integral in Eq. (1) was evaluated over the interval  $[-1, 1]$  and not  $(-\infty, \infty)$ .
- [17] A. Corral and A. Díaz-Guilera, Phys. Rev. E **55**, 2434 (1997).
- [18] I. S. Gradshteyn and I. M. Ryzhik, *Tables of Integrals, Series, and Products* (Academic Press, New York, 1980), Eq. 8.253.1.
- [19] E. Medina, T. Hwa, M. Kardar, and T.-C. Zhang, Phys. Rev. A **39**, 3053 (1989).
- [20] D. Forster, D. R. Nelson, and M. J. Stephen, Phys. Rev. A **16**, 732 (1977).
- [21] T. Sun, M. Plischke, Phys. Rev. E **49**, 5046 (1994).
- [22] A. L. Barabási and H. E. Stanley, *Fractal Concepts in Surface Growth* (Cambridge University Press, Cambridge, England, 1995).
- [23] J. J. Binney, N. J. Dowrick, A. J. Fisher, and M. E. J. Newman, *The Theory of Critical Phenomena* (Oxford University Press, New York, 1992).
- [24] L. Pietronero and W. R. Schneider, Phys. Rev. Lett. **66**, 2336 (1991).
- [25] A. Vespignani, S. Zapperi, and L. Pietronero, Phys. Rev. E **51**, 1711 (1995).
- [26] V. Loreto, L. Pietronero, A. Vespignani, and S. Zapperi, Phys. Rev. Lett. **75**, 465 (1995).